A Computational Study of the Reaction Between N(^{2}D) and Simple Aromatic Hydrocarbons

Marzio Rosi[1,2(✉)], Nadia Balucani[3], Piergiorgio Casavecchia[3], Noelia Faginas-Lago[3], Luca Mancini[3], Dimitrios Skouteris[4], and Gianmarco Vanuzzo[3]

[1] DICA, Università di Perugia, 06125 Perugia, Italy
marzio.rosi@unipg.it
[2] CNR-SCITEC, 06123 Perugia, Italy
[3] DCBB, Università di Perugia, 06123 Perugia, Italy
{nadia.balucani,piergiorgio.casavecchia,
gianmarco.vanuzzo}@unipg.it, luca.mancini@studenti.unipg.it
[4] Master-Tec srl, 06128 Perugia, Italy

Abstract. In this contribution, we will present a computational study of the reactions involving N(^{2}D) and simple aromatic hydrocarbons, like benzene or toluene. The aim is to determine the chemical reactivity of N(^{2}D) with aromatic species after previous investigations with aliphatic molecules, in order to establish which level of calculation is necessary to get reliable results.

Keywords: Computational chemistry · Potential energy surfaces · Ab initio calculations · Density Functional Theory · Coupled Cluster calculations

1 Introduction

The reactivity of atomic nitrogen in its ground state (^{4}S) with closed shell molecules, like hydrocarbons, is very low, while atomic nitrogen in the ^{2}D state is much more reactive with hydrocarbons. N(^{2}D) was detected in the water-poor comet C/2016 R2 (Pan-STARRS) [1] and in a plethora of strongly photon-irradiated environments including the Orion Nebula (M42), low-ionization H II regions (M43), planetary nebulae (*i.e.* the Ring Nebula), supernova remnants (*i.e.* the Crab Nebula), and Herbig-Haro objects [2–5]. Polycyclic aromatic hydrocarbons (PAHs) and related species are presumed to be omnipresent in the interstellar medium (ISM) and aromatic chemistry is widespread in the earliest stages of star formation. Nitrogen, in its molecular form, and hydrocarbons, both aliphatic and aromatic, are also the main components of the atmosphere of Titan [6, 7]. This atmosphere is similar, in some aspects, to the primordial atmosphere of Earth [8, 9] and for this reason has been extensively studied by several missions [10, 11]. Among the hydrocarbons identified on Titan there is benzene [12, 13], while toluene is easily produced by the reaction of C_6H_5, obtained by photodissociation of benzene, and CH_3 [14]. Dinitrogen in the atmosphere of Titan can dissociate into atomic nitrogen both in its ground state or ^{2}D excited state in similar amounts [15, 16] and N (^{2}D) can easily

© The Author(s), under exclusive license to Springer Nature Switzerland AG 2023
O. Gervasi et al. (Eds.): ICCSA 2023 Workshops, LNCS 14105, pp. 718–734, 2023.
https://doi.org/10.1007/978-3-031-37108-0_46

react with other constituents of the upper atmosphere of Titan or with species present in the ISM medium [17–24].

The reaction of N(^{2}D) with several aliphatic hydrocarbons of increasing complexity, starting from methane, have been already investigated both theoretically, using accurate ab initio methods and kinetic calculations, and experimentally through crossed molecular beams techniques [25–32]. A similar approach is employed for the reactions between N(^{2}D) and aromatic hydrocarbons, starting from benzene [33–35] and toluene [36, 37] with the intention to extend the study to more complex aromatic systems, like polycyclic aromatic hydrocarbons (PAHs). In this study we will present the results of calculations performed on the reactions of N(^{2}D) with benzene and toluene paying particular attention to the computational aspects, in order to determine the best approach to the ab initio study of these systems computationally very demanding.

2 Computational Details

The theoretical investigation of the reaction of N(^{2}D) with benzene and toluene was performed adopting a well-established computational strategy previously used for the study of many other bimolecular reactions [38–42]. The optimization of all the stationary points (minima and transition states) was performed at the B3LYP [43, 44] level of theory in conjunction with the 6-311+G(d,p) basis set [45, 46] and, in particular cases, using the ωB97X-D [47, 48] functional with the same 6-311+G(d,p) basis set [45, 46]. The geometry of the optimized stationary points was then refined by the use of the B3LYP functional with a larger basis set, *i.e.* the Dunning aug-cc-pVTZ [49]. The geometry optimizations were always followed by the computation of the vibrational frequencies. IRC calculations [50, 51] were performed to assign the transition states to the relative minima. The energy of all the stationary points was computed then at the CCSD(T) level [52–54] using the aug-cc-pVTZ basis set [49]. All the energies were corrected to 0 K by adding the zero point energy (ZPE) correction computed using the scaled harmonic vibrational frequencies evaluated at the same level of the corresponding geometry optimization. The energy of N(^{2}D) was estimated using the N(^{4}S) – N(^{2}D) experimental energy difference of 55 kcal mol^{-1} [55]. For selected stationary points, very accurate calculations were performed at the CCSD(T) level corrected with a Density Fitted (DF) MP2 extrapolation to the complete basis set (CBS) and with corrections for core electrons excitations. In particular, we compute the energies as:

ECBS = E(CCSD(T)/aug-cc-pVTZ) + [E(CCSD(T,core)/cc-pVTZ)-E(CCSD(T)/cc-pVTZ)] + [E(DF-MP2/CBS)-E(DF-MP2/aug-cc-pVTZ)]

where E(DF-MP2/CBS) is defined as:

E(DF-MP2/CBS) = E[(DF-MP2)/aug-cc-pVQZ)] + 0.5772*[E(DF-MP2/aug-cc-pVQZ)-E(DF-MP2/aug-cc-pVTZ)]

The E(DF-MP2/CBS) extrapolation was performed using Martin's two parameter scheme [56]. These energies will be denoted as CBS although they include also the core-valence correlation correction. The accuracy of these calculations should be within ± 1 kcal mol^{-1}.

The DFT and CCSD(T) calculations were done using Gaussian 09 [57] while the CBS calculations were done with MOLPRO [58, 59]. Molekel was used for the analysis of the optimized structures and the vibrational frequencies [60, 61].

3 Results and Discussion

3.1 Attack of N(^{2}D) to the Aromatic Ring

Table 1 reports the energy difference between the energy of atomic nitrogen in its ^{4}S ground state and in its first excited ^{2}D state. As expected, the description of a lowest spin excited state is a difficult task and the results obtained with a single-reference method are unsatisfactory. In particular, we have an error of 9 kcal mol^{-1} at B3LYP level using a split valence basis set, which is reduced to 8 kcal mol^{-1} using a more extended basis set like the aug-cc-pVTZ. Using a method which includes more extensively correlation effects like the CCSD(T) does not improve significantly the description, being the error still 7 kcal mol^{-1}. Even a very accurate method wich includes at CCSD(T) level an extrapolation to the complete basis set and the core-valence correlation effects, *i.e.* the CBS scheme, provides an unsatisfactory description, being the error still 6 kcal mol^{-1}. For this reason, we decided to evaluate the energy of N (^{2}D) adding the experimental energy difference to N(^{4}S) which is well described at any level of approximation. The energy of nitrogen in its excited ^{2}D state will be estimated in this way in all the calculations.

Table 1. Total energy (hartree) and energy differences **Δ** (kcal mol^{-1}) between nitrogen in its ground ^{4}S state and in the ^{2}D state computed at various level of calculation compared to the experimental value [56].

Method	N(^{4}S)	N(^{2}D)	Δ
B3LYP/6-311+G(d,p)	−54.600723	−54.499263	64
B3LYP/aug-cc-pVTZ	−54.602891	−54.502416	63
CCSD(T)/aug-cc-pVTZ	−54.516924	−54.417503	62
CBS	−54.585385	−54.488412	61
Experiment			55

The approach of N(^{2}D) to benzene leads first of all to the formation of an adduct where the distance between the nitrogen atom and the benzene ring is very long, more than 3 Å. In Fig. 1 we have reported the optimized geometry computed at B3LYP/aug-cc-pVTZ level for the initial adduct derived from the interaction of N(^{2}D) with benzene and toluene; for benzene we have performed the geometry optimization also at ωB97XD/6-311+G(d,p) (parameters reported in red in parentheses) and from Fig. 1 we can notice that no significative differences in the optimized parameters are present.

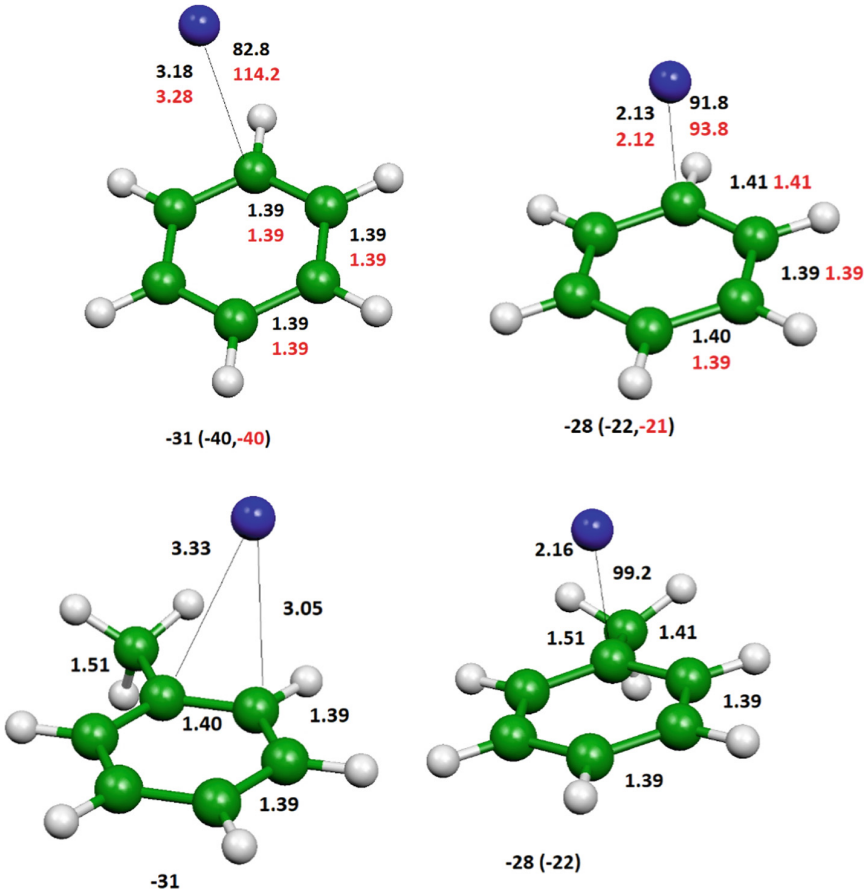

Fig. 1. Optimized structures of the initial adduct obtained for the attack of N(^{2}D) to benzene (top) or toluene (bottom) and the transition state for the isomerization of the adduct to the first stable species. Geometry optimization has been performed at B3LYP/aug-cc-pVTZ (in black) and ωB97X-D/6-311+G(d,p) (in red) level. Bond lengths in Å, angles in degrees. Relative energies (kcal mol^{-1}) with respect to N(^{2}D) + aromatic ring have been evaluated at B3LYP/aug-cc-pVTZ and, in parentheses, at CCSD(T)/aug-cc-pVTZ//B3LYP/aug-cc-pVTZ and CCSD(T)/aug-cc-pVTZ//ωB97X-D/6-311+G(d,p) (in red) level of theory. Carbon atoms in green, nitrogen in blue, hydrogen in white. (Color figure online)

The nitrogen atom approaches the ring almost in a perpendicular way, being the NCH angle 82.8° at B3LYP/aug-cc-pVTZ level and 114.2° at ωB97XD/6-311+G(d,p) level. Due to the very long distance between the nitrogen atom and the aromatic ring, the geometry of benzene is almost unchanged with respect to that of isolated benzene. This electrostatic adduct evolves to the first intermediate, **w1**, through the transition state shown in Fig. 1. The geometry of this saddle point is very close to that of the adduct, the only significant difference being the N—C distance which changes from 3.18 to 2.13 Å. Although the optimized geometries seem to be reasonable, the relative energies of these species with respect to the reactants are not. The adduct is more stable with respect to the reactants by 31 kcal mol^{-1} at B3LYP/aug-cc-pVTZ level and by 40 kcal mol^{-1} at CCSD(T)/aug-cc-pVTZ level using both the B3LYP/aug-cc-pVTZ or the ωB97XD/6-311+G(d,p) optimized geometries. This energy does not seem to be correct, since an electrostatic adduct where the interaction between the two species is very weak cannot be stabilized so strongly. The energy of this adduct is so low with respect to the reactants because in this species there is a very bad description of $N(^2D)$, which is almost not interacting with benzene, which lowers unrealistically the energy of the adduct. This adduct is formed by a nitrogen atom and a benzene ring almost not interacting; its energy should be almost equal to the sum of the energies of $N(^2D)$ and C_6H_6. Also the energy of the transition state is too low with respect to the reactants being 28 kcal mol^{-1} under the reactants and 22 or 21 kcal mol^{-1} at CCSD(T)/aug-cc-pVTZ level, depending on the use of the optimized geometry at B3LYP/aug-cc-pVTZ or ωB97XD/6-311+G(d,p) level. In order to solve this problem, we computed the energy of both species, minimum and saddle point, at CBS level. The energy of the adduct was computed to be 4 kcal mol^{-1} over the reactants starting from the B3LYP/aug-cc-pVTZ optimized geometry and 5 kcal mol^{-1} over the reactants using the ωB97XD/6-311+G(d,p) geometry. This point suggests that the description of the initial attack of $N(^2D)$ to benzene cannot be described properly at this level of calculation. Multirefence methods, as CASPT2 for instance, should be employed, but their use could be too computer resources demanding for systems as big as the ones here considered. A more affordable alternative could be the use of semiempirical methods, as the Improved Lennard-Jones (ILJ) which provides realistic description of long range interactions [62–65]. Since we are interested in the exit channels and relative branching factors of the investigated reactions we decided to considered the reaction starting from the first intermediate, *i.e.* species **w1**, as previously done by Chin et al. [66].

The interaction of $N(^2D)$ with toluene shows a behaviour similar to that of benzene. In Fig. 1 we can see the formation of an initial adduct where the nitrogen atom is very far from the toluene ring (more than 3 Å) and the toluene ring is almost unperturbed. This species is more stable than the reactants by 31 kcal mol^{-1} at B3LYP/aug-cc-pVTZ level (the CCSD(T) calculation did not converge). Also the transition state lies under the reactants by 28 kcal mol^{-1} at B3LYP/aug-cc-pVTZ level and 22 kcal mol^{-1} at CCSD(T)/aug-cc-pVTZ level. These energies clearly overestimate the strength of the interaction between the nitrogen atom and the toluene molecule. Also in this case this description cannot be considered correct and, therefore, we will start our analysis for this reaction starting from the first intermediate, *i.e.* **w1**.

3.2 Interaction of N(^{2}D) with Benzene

We will focus our attention only to the main reactive channel, *i.e.* the one leading to the formation of hydrogen cyanide and the cyclopentadienyl radical, since we are interested in computational requirements. The other reactive channels have been reported elsewhere [34–36]. The potential energy surface (PES) relative to this reaction channel is reported in Fig. 2, while the optimized geometries of the intermediates and transition states considered in Fig. 2 are reported in Fig. 3 and 4, respectively. We can notice from Fig. 2 that the first intermediate is species **w1** where the nitrogen is bonded to a carbon atom of the ring, together with an hydrogen atom. This carbon center therefore changes its hybridization from sp^2 to sp^3 and the ring is distorted. This attack to a carbon of the ring is in agreement with the structure of the initial adduct reported in Fig. 1. Species **w1** can evolve towards the products following two different pathways: the first (in red) implies the evolution of **w1** through **w2**, **w4**, **w6**, **w9**, while the second (in blue) implies a pathway which goes through **w3**, **w5**, **w7**, **w8**, **w9**. The second pathway shows the presence of an initial saddle point higher in energy. However, in order to establish which one is the preferred pathway kinetic calculations are necessary and they have been presented elsewhere [36].

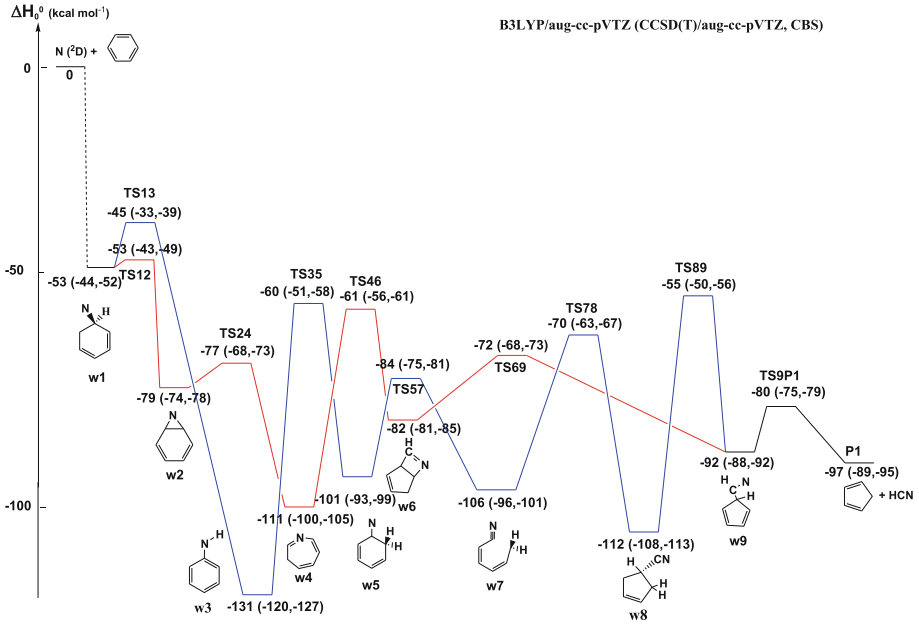

Fig. 2. PES for two of the main reaction pathways of the N(^{2}D) + benzene reaction. Relative energies (kcal mol^{-1}) respect to N(^{2}D) + benzene, computed at B3LYP, CCSD(T) (in parentheses, first entry) and CBS (in parentheses, second entry) level with inclusion of ZPE.

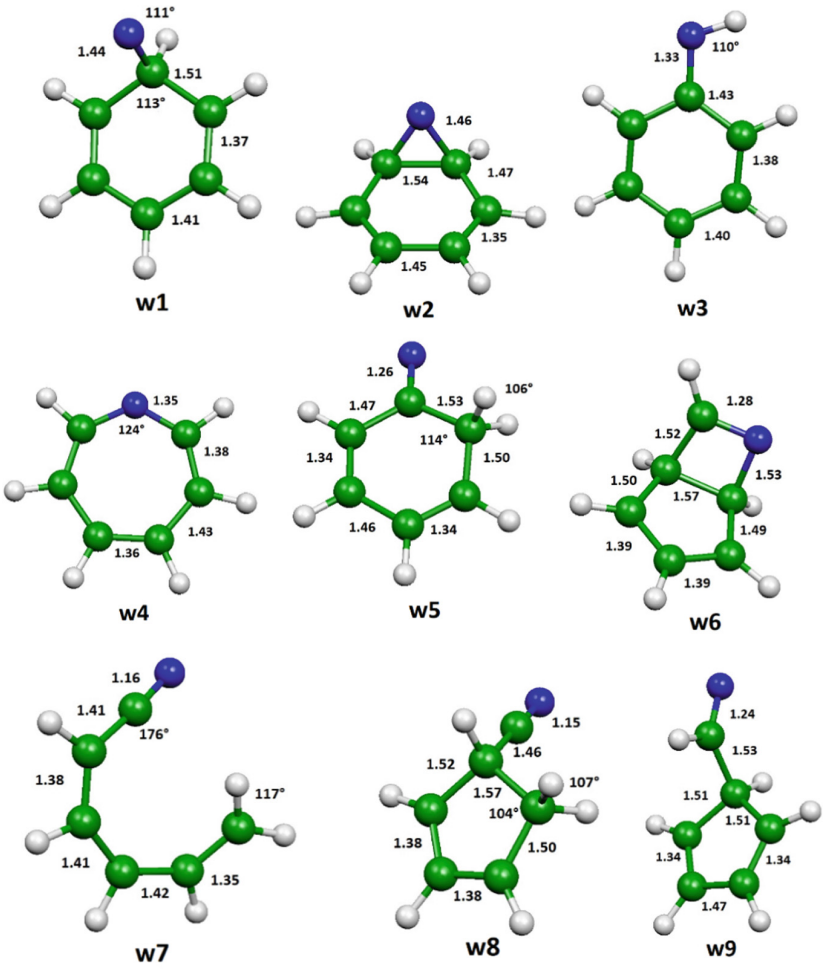

Fig. 3. Optimized geometries of the minima reported in Fig. 2. Geometry optimization has been performed at B3LYP level. Distances in Å, angles in °. Carbon atoms in green, nitrogen in blue, hydrogen in white. (Color fgure online)

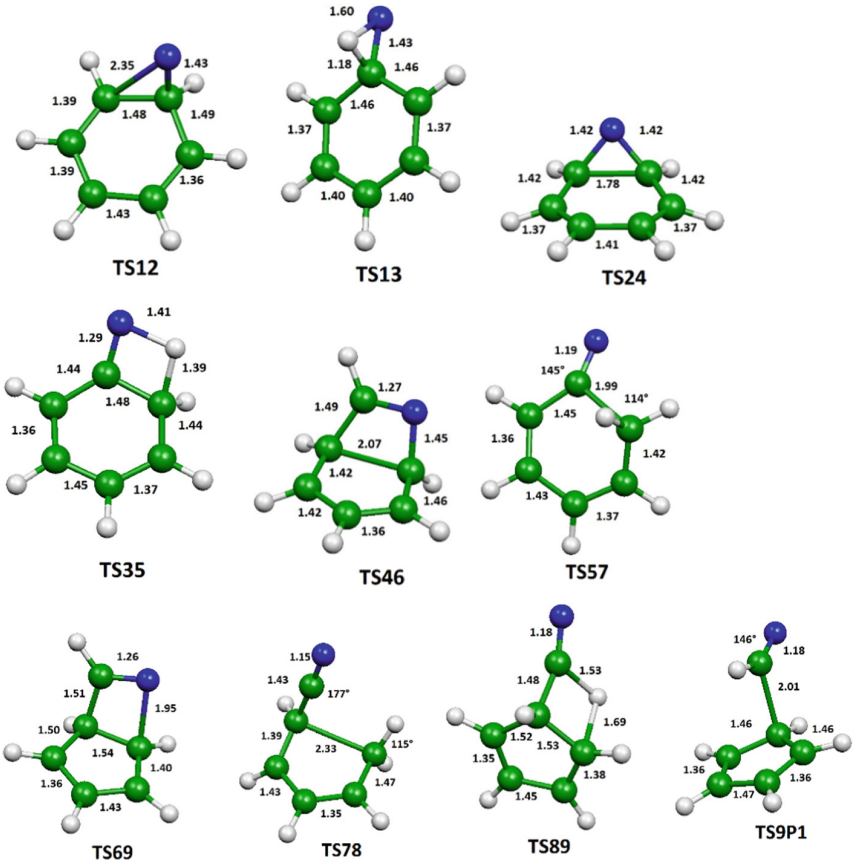

Fig. 4. Optimized geometries of the transition states reported in Fig. 2. Geometry optimization has been performed at B3LYP level. Distances in Å, angles in °. Carbon atoms in green, nitrogen in blue, hydrogen in white. (Color fgure online)

For each stationary point we have reported the energy computed at B3LYP/aug-cc-pVTZ, CCSD(T)/aug-cc-pVTZ and CBS level. We can notice that there are significant differences among the three approaches. In particular we can notice that there is an overestimation of the binding energies at B3LYP level as expected, and an underestimation of the binding energies at CCSD(T) level due to the basis set incompleteness. These two errors somehow cancel each other, with the result that the B3LYP energies are closer to the CBS ones, than the CCSD(T) energies. However, if we change the reference energy, considering that of the first intermediate **w1**, the difference among the energies of the three methods considered are lower, as we can see from Fig. 5, suggesting that also the B3LYP method can provide reasonable semi-quantitative results, also for energies besides those for geometries. This is encouraging in view of the possible investigation of more complex systems. The comparison between the energies computed at CCSD(T)/aug-cc-pVTZ and CBS level allows us to estimate the absolute basis set

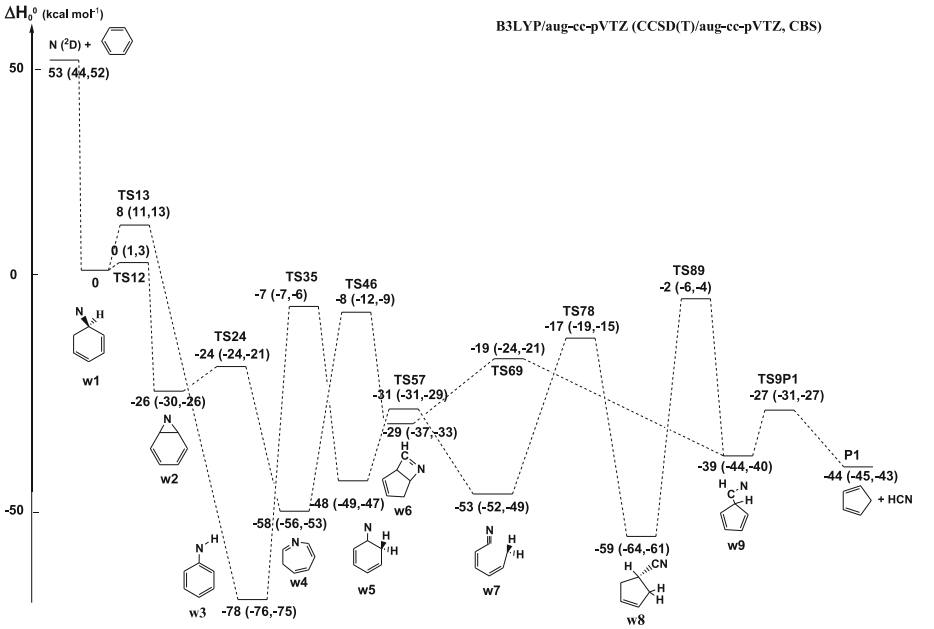

Fig. 5. PES for two of the main reaction pathways of the N(^{2}D) + benzene reaction. Relative energies (kcal mol^{-1}) respect to **w1** intermediate, computed at B3LYP, CCSD(T) (in parentheses, first entry) and CBS (in parentheses, second entry) level with inclusion of ZPE.

superposition error (BSSE) which is around 3–4 kcal/mol. However, this error is not so relevant as far as we are interested in relative energies.

3.3 Interaction of N(^{2}D) with Toluene

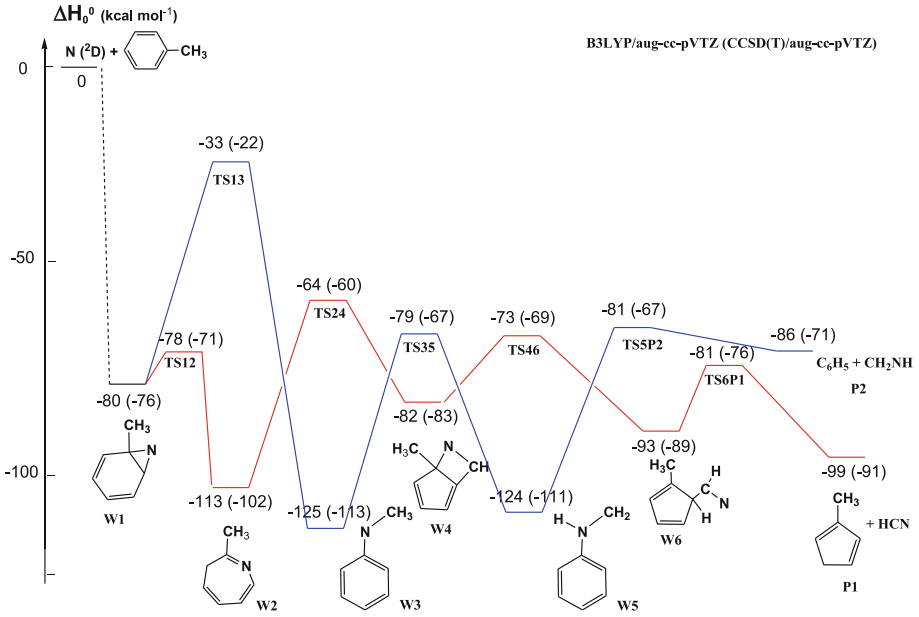

Fig. 6. PES for two of the main reaction pathways of the N(^{2}D) + toluene reaction. Relative energies (kcal mol^{-1}), respect to N(^{2}D) + toluene, are computed at B3LYP and CCSD(T) (in parentheses) level with inclusion of ZPE.

Figure 6 shows the PES of the reaction between N(^{2}D) and toluene, while the optimized structures of the minima and transition states are reported in Figs. 7 and 8, respectively. Also in this case we have considered only the channel leading to the formation of hydrogen cyanide, since the other reaction channels will be presented elsewhere. For analogy with the reaction of benzene we have considered also the evolution of intermediate **w3**, which in this case however leads to different products. The first intermediate, **w1**, shows the nitrogen center bonded η^2 to two carbon atoms; this is in agreement with the optimized structure of the initial adduct reported in Fig. 1, where it is clear that the nitrogen atom approaches two carbon atoms. From Fig. 6 we can see that species **w1** can evolve to the formation of hydrogen cyanide and methylcyclopentadyenil radical through the intermediates **w2**, **w4** and **w6** (red pathway). **w1** can isomerize also to **w3**, which is the species corresponding to the intermediate **w3** in the PES of N(^{2}D) + benzene. However, this species shows a different reactivity since the migration of an hydrogen of the CH_3 group to the nitrogen is preferred with respect to the migration of the whole CH_3 group to the adjacent carbon atom of the benzene ring. **w3** can dissociate into a phenyl radical and methanimine. Fron Fig. 6, where we have reported the energies relative to the reactants computed at B3LYP/aug-cc-pVTZ and CCSD(T)/aug-cc-pVTZ (in parentheses) levels, we can notice significant differences between the values obtained with the two methods. In Fig. 9 we have reported the PES changing the reference energy. Also

in this case we can notice that there is a smaller difference between the two methods. However, it seems clear that for a quantitative treatment at least CCSD(T) calculations are necessary. B3LYP can provide reasonable semi-quantitative results which anyway can be important when other methods are unfeasible.

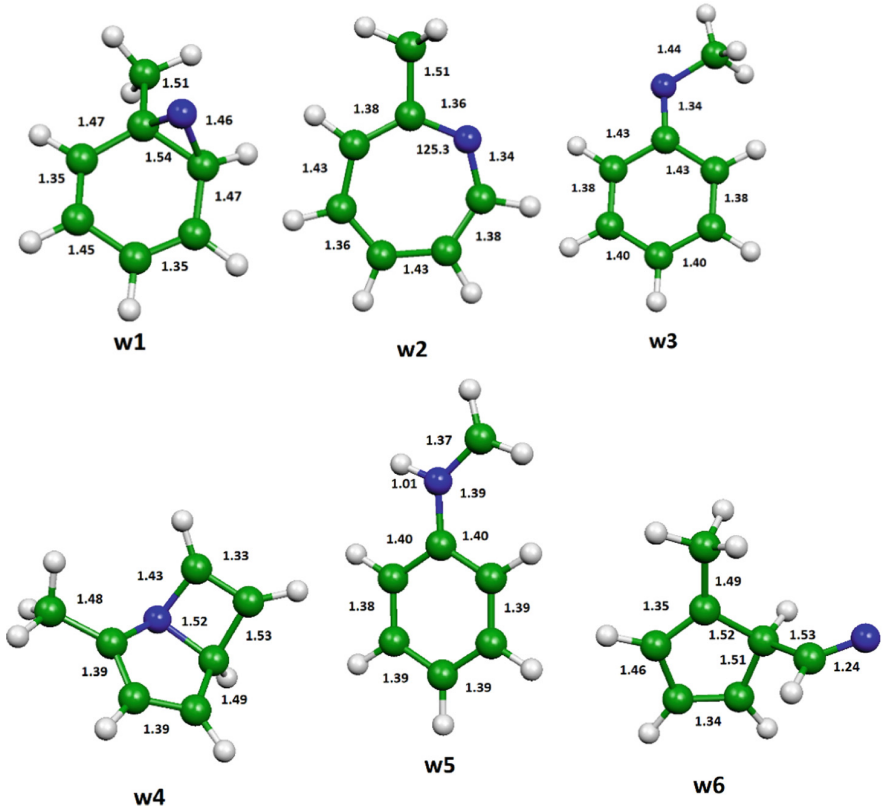

Fig. 7. Optimized geometries of the minima reported in Fig. 6. Geometry optimization has been performed at B3LYP/aug-cc-pVTZ level. Distances in Å, angles in °. Carbon atoms in green, nitrogen in blue, hydrogen in white. (Color fgure online)

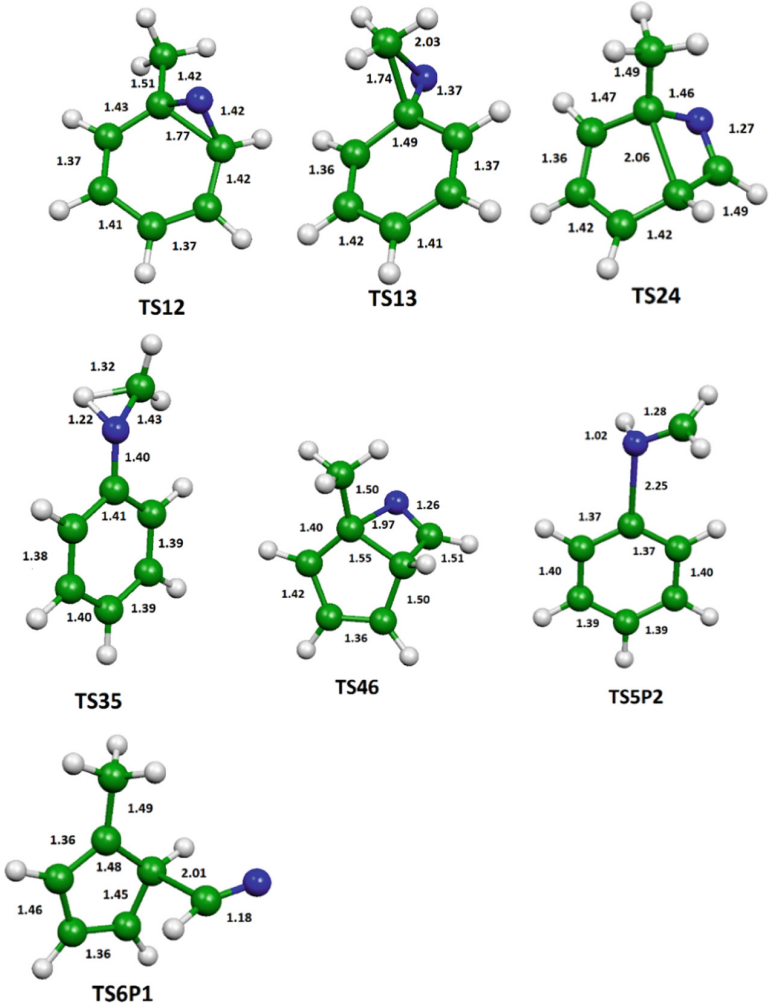

Fig. 8. Optimized geometries of the transition states reported in Fig. 6. Geometry optimization has been performed at B3LYP/aug-cc-pVTZ level. Distances in Å, angles in °. Carbon atoms in green, nitrogen in blue, hydrogen in white. (Color fgure online)

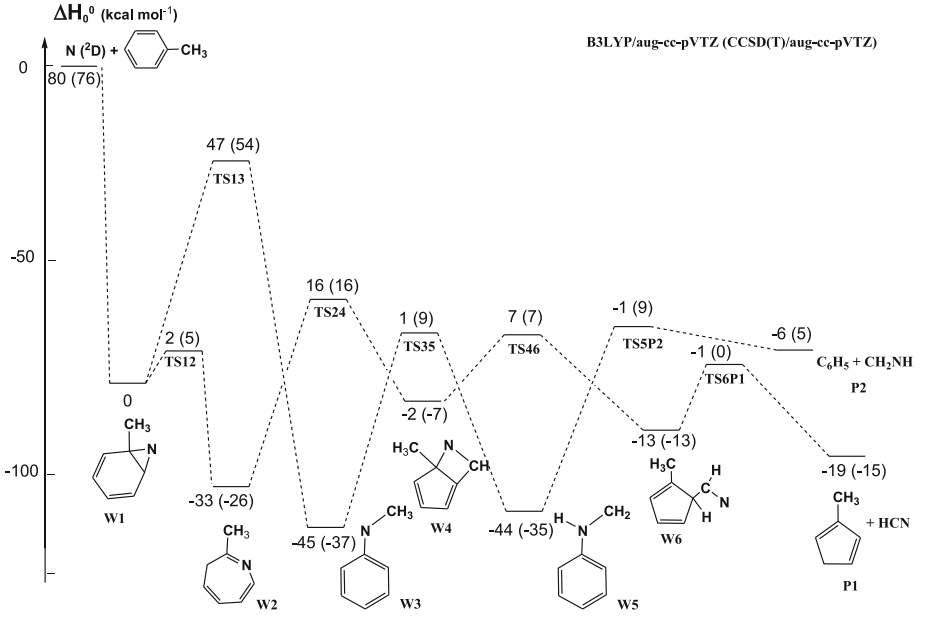

Fig. 9. PES for two of the main reaction pathways of the N(^{2}D) + toluene reaction. Relative energies (kcal mol^{-1}), respect to **w1** species, are computed at B3LYP and CCSD(T) (in parentheses) level with inclusion of ZPE.

4 Conclusions

The theoretical investigation of the interaction of N(^{2}D) with benzene and toluene, focusing the attention on computational requirements, suggests that a quantitative treatment of these reactions requires extensive inclusion of correlation effects as well as extrapolation to the basis set completeness limit. Particularly challenging is the initial approach of N(^{2}D) to the aromatic system, which cannot be described properly by single reference methods. Multireference methods, which could be unfeasible for most of the aromatic systems, should be employed, although an alternative worth of consideration could be represented by semiempirical methods which describe properly long range interactions. The comparison between DFT and CCSD(T) calculations suggests that useful semi-quantitative results can be obtained also at DFT level of approximation. This is an important result in order to extend our study to complex PAHs.

Acknowledgments. The authors acknowledge the MUR (Italian Ministry of University and Research) for "PRIN 2017" funds, project "MAGIC DUST" (Prot. 2017PJ5XXX_002).

References

1. Raghuram, S., Hutsemékers, D., Opitom, C., Jehin, E., Bhardwaj, A., Manfroid, J.: Forbidden atomic carbon, nitrogen, and oxygen emission lines in the water-poor comet C/2016 R2 (Pan-STARRS). Astron. Astrophys. **635**, A108 (2020)

2. Ferland, G.J., Henney, W.J., O'Dell, C.R., Porter, R.L., van Hoof, P.A.M., Williams, R.J.R.: Pumping up the [N i] nebular lines. Astrophys. J. **757**, 79 (2012)
3. Dopita, M.A., Mason, D.J., Robb, W.D.: Atomic nitrogen as a probe of physical conditions in the interstellar medium. Astrophys. J. **207**, 102–109 (1976)
4. Ferland, G.J., Rees, M.J.: radiative equilibrium of high-density clouds, with application to active galactic nucleus continua. Astrophys. J. **332**, 141 (1988)
5. Bautista, M.A.: Continuum fluorescence excitation of [N I] and [O I] lines in gaseous nebulae. Astrophys. J. **527**, 474 (1999)
6. Hörst, S.M.: Titan's atmosphere and climate. J. Geophys. Res.: Planets **122**, 432–482 (2017)
7. Vuitton, V., Yelle, R.V., Anicich, V.G.: The nitrogen chemistry of Titan's upper atmosphere revealed. Astrophys J. **647**, L175–L178 (2006)
8. Vuitton, V., Dutuit, O., Smith, M.A., Balucani, N.: Chemistry of Titan's atmosphere. In: Mueller-Wodarg, I., Griffith, C., Lellouch, E., Cravens, T. (eds.) Titan: Surface. Atmosphere and Magnetosphere. Cambridge University Press, Cambridge (2013)
9. Balucani, N.: Elementary reactions of N atoms with hydrocarbons: first steps towards the formation of prebiotic N-containing molecules in planetary atmospheres. Chem. Soc. Rev. **41**, 5473–5483 (2012)
10. Brown, R., Lebreton, J.P., Waite, J. (eds.): Titan from Cassini-Huygens. Springer, Netherlands (2010)
11. Lai, J.C.-Y., et al.: Mapping vinyl cyanide and other nitriles in Titan's atmosphere using ALMA. Astron. J. **154**(206), 1–10 (2017)
12. Vuitton, V., Yelle, R.V., Cui, J.: Formation and distribution of benzene on Titan. J. Geophys. Res. **113**, E05007 (2008)
13. Clark, R.N., et al.: Detection and mapping of hydrocarbon deposits on Titan. J. Geophys. Res. **115**, E10005 (2010)
14. Loison, J.C., Dobrijevic, M., Hickson, K.M.: The photochemical production of aromatics in the atmosphere of Titan. Icarus **329**, 55–71 (2019)
15. Lavvas, P., et al.: Energy deposition and primary chemical products in Titan's upper atmosphere. Icarus **213**, 233–251 (2011)
16. Dutuit, O., et al.: Critical review of N, N^+, N_2^+, N^{++} and N_2^{++} main production processes and reactions of relevance to Titan's atmosphere. Astrophys. J. Suppl. Ser. **204**, 20 (2013)
17. Balucani, N.: Nitrogen fixation by photochemistry in the atmosphere of Titan and implications for prebiotic chemistry. In: Trigo-Rodriguez, J.M., Raulin, F., Muller, C., Nixon, C. (eds.) The Early Evolution of the Atmospheres of Terrestrial Planets. Springer Series in Astrophysics and Space Science Proceedings, vol. 35, pp. 155–164. Springer, New York (2013). https://doi.org/10.1007/978-1-4614-5191-4_12
18. Balucani, N.: Elementary reactions and their role in gas-phase prebiotic chemistry. Int. J. Mol. Sci. **10**, 2304–2335 (2009)
19. Imanaka, H., Smith, M.A.: Formation of nitrogenated organic aerosols in the Titan upper atmosphere. PNAS **107**, 12423–12428 (2010)
20. Balucani, N., et al.: Dynamics of the N(^{2}D) + D_2 reaction from crossed-beam and quasiclassical trajectory studies. J. Phys. Chem. A **105**, 2414–2422 (2001)
21. Balucani, N., et al.: Experimental and theoretical differential cross sections for the N(^{2}D) + H_2 reaction. J. Phys. Chem. A **110**, 817–829 (2006)
22. Homayoon, Z., Bowman, J.M., Balucani, N., Casavecchia, P.: Quasiclassical trajectory calculations of the N(^{2}D) + H_2O reaction elucidating the formation mechanism of HNO and HON seen in molecular beam experiments. J. Phys. Chem. Lett. **5**, 3508–3513 (2014)
23. Balucani, N., Cartechini, L., Casavecchia, P., Homayoon, Z., Bowman, J.M.: A combined crossed molecular beam and quasiclassical trajectory study of the Titan-relevant N(^{2}D) + D_2O reaction. Mol. Phys. **113**, 2296–2301 (2015)

24. Israel, G., et al.: Complex organic matter in Titan's atmospheric aerosols from in situ pyrolysis and analysis. Nature **438**, 796 (2005)
25. Balucani, N., et al.: Combined crossed molecular beam and theoretical studies of the N(^{2}D) + CH_4 reaction and implications for atmospheric models of Titan. J. Phys. Chem. A **113**, 11138–11152 (2009)
26. Balucani, N., et al.: Cyanomethylene formation from the reaction of excited nitrogen atoms with acetylene: a crossed beam and ab initio study. J. Am. Chem. Soc. **122**, 4443–4450 (2000)
27. Balucani, N., Cartechini, L., Alagia, M., Casavecchia, P., Volpi, G.G.: Observation of nitrogen-bearing organic molecules from reactions of nitrogen atoms with hydrocarbons: a crossed beam study of N(^{2}D) + ethylene. J. Phys. Chem. A **104**, 5655–5659 (2000)
28. Balucani, N., et al.: Formation of nitriles and imines in the atmosphere of Titan: combined crossed-beam and theoretical studies on the reaction dynamics of excited nitrogen atoms N(^{2}D) with ethane. Faraday Discuss. **147**, 189–216 (2010)
29. Balucani, N., et al.: Combined crossed beam and theoretical studies of the N(^{2}D) + C_2H_4 reaction and implications for atmospheric models of Titan. J. Phys. Chem. A **116**, 10467–10479 (2012)
30. Vanuzzo, G., et al.: Reaction N(^{2}D) + CH_2CCH_2 (Allene): an experimental and theoretical investigation and implications for the photochemical models of Titan. ACS Earth Space Chem. **6**, 2305–2321 (2022)
31. Mancini, L., et al.: The reaction N(^{2}D) + CH_3CCH (Methylacetylene): a combined crossed molecular beams and theoretical investigation and implications for the atmosphere of titan. J. Phys. Chem A **125**, 8846–8859 (2021)
32. Mancini, L., de Aragão, E.V.F., Rosi, M., Skouteris, D., Balucani, N.: A theoretical investigation of the reactions of N(^{2}D) with small alkynes and implications for the prebiotic chemistry of titan. In: Gervasi, O., et al. (eds.) ICCSA 2020. LNCS, vol. 12251, pp. 717–729. Springer, Cham (2020). https://doi.org/10.1007/978-3-030-58808-3_52
33. Balucani, N., Pacifici, L., Skouteris, D., Caracciolo, A., Casavecchia, P., Rosi, M.: A theoretical investigation of the reaction N(2D) + C6H6 and implications for the upper atmosphere of Titan. In: Gervasi, O., et al. (eds.) ICCSA 2018. LNCS, vol. 10961, pp. 763–772. Springer, Cham (2018). https://doi.org/10.1007/978-3-319-95165-2_53
34. Balucani, N., et al.: A Computational Study of the Reaction N(^{2}D) + C_6H_6 Leading to Pyridine and Phenylnitrene. In: Misra, S., et al. (eds.) ICCSA 2019. LNCS, vol. 11621, pp. 316–324. Springer, Cham (2019). https://doi.org/10.1007/978-3-030-24302-9_23
35. Balucani, N., et al.: An experimental and theoretical investigation of the N(^{2}D) + C_6H_6 (benzene) reaction with implications for the photochemical models of Titan. Faraday Discuss. (2023). https://doi.org/10.1039/D3FD00057E
36. Rosi, M., et al.: A computational study on the attack of nitrogen and oxygen atoms to toluene. In: Gervasi, O., et al. (eds.) ICCSA 2021. LNCS, vol. 12953, pp. 620–631. Springer, Cham (2021). https://doi.org/10.1007/978-3-030-86976-2_42
37. Rosi, M., et al.: A computational study on the insertion of N(^{2}D) into a C—H or C—C bond: the reactions of N(^{2}D) with benzene and toluene and their implications on the chemistry of titan. In: Gervasi, O., et al. (eds.) ICCSA 2020. LNCS, vol. 12251, pp. 744–755. Springer, Cham (2020). https://doi.org/10.1007/978-3-030-58808-3_54
38. Balucani, N., Skouteris, D., Ceccarelli, C., Codella, C., Falcinelli, S., Rosi, M.: A theoretical investigation of the reaction between the amidogen, NH, and the ethyl, C_2H_5, radicals: a possible gas-phase formation route of interstellar and planetary ethanimine. Molec. Astrophys. **13**, 30–37 (2018)
39. Sleiman, C., El Dib, G., Rosi, M., Skouteris, D., Balucani, N., Canosa, A.: Low temperature kinetics and theoretical study of the reaction CN + CH_3NH_2: a potential source of cyanamide and methyl cyanamide in the interstellar medium. PCCP **20**, 5478–5489 (2018)

40. Berteloite, C., et al.: Low temperature kinetics, crossed beam dynamics and theoretical studies of the reaction S(^{1}D) + CH_4 and low temperature kinetics of S(^{1}D) + C_2H_2. Phys. Chem. Chem. Phys. **13**, 8485–8501 (2011)
41. Rosi, M., et al.: Possible scenarios for SiS formation in the interstellar medium: electronic structure calculations of the potential energy surdaces for the reactions of the SiH radical with atomic sulphur and S_2. Chem. Phys. Lett. **695**, 87–93 (2018)
42. Troiani, A., Rosi, M., Garzoli, S., Salvitti, C., de Petris, G.: Vanadium hydroxide cluster ions in the gas phase: bond-forming reactions of doubly-charged negative ions by SO_2-promoted V-O activation. Chem. Eur. J. **23**, 11752–11756 (2017)
43. Becke, A.D.: Density functional thermochemistry. III. The role of exact exchange. J. Chem. Phys. **98**, 5648–5652 (1993)
44. Stephens, P.J., Devlin, F.J., Chablowski, C.F., Frisch, M.J.: Ab initio calculation of vibrational absorption and circular dichroism spectra using density functional force fields. J. Phys. Chem. **98**, 11623–11627 (1994)
45. Krishnan, R., Binkley, J.S., Seeger, R., Pople, J.A.: Self-consistent molecular orbital methods. XX. A basis set for correlated wave functions. J. Chem. Phys. **72**, 650–654 (1980)
46. Frisch, M.J., Pople, J.A., Binkley, J.S.: Self-consistent molecular orbital methods 25. Supplementary functions for Gaussian basis sets. J. Chem. Phys. **80**, 3265–3269 (1984)
47. Chai, J.-D., Head-Gordon, M.: Long-range corrected hybrid density functionals with damped atom-atom dispersion corrections. Phys. Chem. Chem. Phys. **10**, 6615–6620 (2008)
48. Chai, J.-D., Head-Gordon, M.: Systematic optimization of long-range corrected hybrid density functionals. J. Chem. Phys. **128**, 084106 (2008)
49. Dunning, T.H., Jr.: Gaussian basis sets for use in correlated molecular calculations. I. The atoms boron through neon and hydrogen. J. Chem. Phys. **90**, 1007–1023 (1989)
50. Gonzalez, C., Schlegel, H.B.: An improved algorithm for reaction path following. J. Chem. Phys. **90**, 2154–2161 (1989)
51. Gonzalez, C., Schlegel, H.B.: Reaction path following in mass-weighted internal coordinates. J. Phys. Chem. **94**, 5523–5527 (1990)
52. Bartlett, R.J.: Many-body perturbation theory and coupled cluster theory for electron correlation in molecules. Annu. Rev. Phys. Chem. **32**, 359–401 (1981)
53. Raghavachari, K., Trucks, G.W., Pople, J.A., Head-Gordon, M.: Quadratic configuration interaction. A general technique for determining electron correlation energies. Chem. Phys. Lett. **157**, 479–483 (1989)
54. Olsen, J., Jorgensen, P., Koch, H., Balkova, A., Bartlett, R.J.: Full configuration–interaction and state of the art correlation calculations on water in a valence double-zeta basis with polarization functions. J. Chem. Phys. **104**, 8007–8015 (1996)
55. Moore, C.E.: Atomic energy levels. Natl. Bur. Stand. (U.S.) Circ. N. 467. U.S., GPO, Washington, DC (1949)
56. Martin, J.M.: Ab initio total atomization energies of small molecules—towards the basis set limit. Chem. Phys. Lett. **259**, 669–678 (1996)
57. Frisch, M.J., et al.: Gaussian, Inc., Wallingford CT (2009)
58. Werner, H.-J., Knowles, P.J., Knizia, G., Manby, F.R., Schütz, M.: Molpro: a general-purpose quantum chemistry program package. WIREs Comput. Mol. Sci. **2**, 242–253 (2012)
59. Werner, H.-J., et al.: The Molpro quantum chemistry package. J. Chem. Phys. **152**, 144107 (2020)
60. Flükiger, P., Lüthi, H.P., Portmann, S., Weber, J.: MOLEKEL 4.3, Swiss Center for Sci-entific Computing, Manno (Switzerland) (2000–2002)
61. Portmann, S., Lüthi, H.P.: MOLEKEL: an interactive molecular graphics tool chimia, vol. 54, pp. 766–769 (2000)
62. Richardson, V., et al.: Fragmentation of interstellar methanol by collisions with $He.^+$: an experimental and computational study. PCCP **24**, 22437–22452 (2022)

63. de Aragao, E.V.F., Mancini, L., Faginas-Lago, N., Rosi, M., Skouteris, D., Pirani, F.: Semiempirical potential in kinetics calculations on the HC_3N + CN reaction. Molecules **27**, 2297 (2022)
64. de Aragão, E.V.F., et al.: Coding cross sections of an electron charge transfer process. In: Gervasi, O., Murgante, B., Misra, S., Rocha, A.M.A.C., Garau, C. (eds.) ICCSA 2022. LNCS, vol. 13382, pp. 319–333. Springer, Cham (2022). https://doi.org/10.1007/978-3-031-10592-0_24
65. de Aragao, E.V.F., Mancini, L., Faginas-Lago, N., Rosi, M., Balucani, N., Pirani, F.: Long-range complex in the HC_3N + CN potential energy surface: ab initio calculations and intermolecular potential. In: Gervasi, O., et al. (eds.) ICCSA 2021. LNCS, vol. 12958, pp. 413–425. Springer, Cham (2021). https://doi.org/10.1007/978-3-030-87016-4_31
66. Chin, C.-H., Zhu, T., Zhang, J.Z.H.: Cyclopentadienyl radical formation from the reaction of excited nitrogen atoms with benzene: a theoretical study. PCCP **23**, 12408–12420 (2021)